Anal. Chem. **2003,** *75,* 978−985

On-Line Multibed Sorption Trap and Injector for the GC Analysis of Organic Vapors in Large-Volume Air Samples

Juan M. Sanchez and Richard D. Sacks*

Department of Chemistry, University of Michigan, Ann Arbor, Michigan 48109

A capillary-dimension on-line sorption trap is used to preconcentrate organic vapors from large-volume air samples and inject the organic compounds into the separation column as a relatively narrow vapor plug. The multibed trap is made from a Co−Ni alloy for resistive heating during sample desorption and uses four different carbon-based adsorption materials that are graded from weakest to strongest in the direction of the sample gas flow during sample preconcentration. The flow direction then is reversed for sample injection. The multibed design and the flow direction reversal during thermal desorption prevents the higher-boiling-point compounds in the sample from reaching the strongest adsorbing material, from which they would be difficult to desorb as a sufficiently narrow vapor plug. A relatively high current pulse is used to rapidly achieve trap temperatures in the 200−400 °C temperature range, and a lower current is used to maintain the maximum temperature for several seconds in order to ensure injection of the entire trapped sample. A temperature of 350 °C is reached after ∼1.5 s, and injection plug widths are typically in the range of 0.6−1.3 s. Plots of peak area versus sample collection time show excellent linearity and shot-to-shot relatively standard deviations of about ±5%. Performance data are presented for a mixture of 42 volatile compounds spanning a volatility range from *n*-C_5 to *n*-C_{12}. Data are presented for injection plug width and shape for both polar and nonpolar compounds. Decomposition of thermally labile compounds is observed for injection temperatures above 300 °C.

Accurate determination of volatile organic compounds (VOCs) at trace levels in ambient air and gaseous samples is of great interest because they are key components in industrial, environmental, indoor and outdoor air, and medical samples.[1−4] Sampling of VOCs in ambient air is typically performed off-line with air samplers (i.e., canister or sorbent traps) followed by a laboratory analysis using GC or GC/MS.[4−7] Canister sampling techniques are more expensive than sorbent-trap techniques. Moreover, handling is complicated and requires sophisticated equipment for cleaning.[4,5,8]

Sorbent-trap techniques have many advantages over canister sampling, but the need to store samples between sampling and subsequent analysis in the laboratory results in some problems. An important source of error when sorbent traps are used is the formation of artifacts caused by degradation reactions of both adsorbed analytes and the adsorbent itself during storage of adsorbent tubes.[9−11] In addition, strict requirements for a narrow injection plug for GC analysis make a second preconcentration step necessary to refocus the solutes on the analytical column. This is frequently done by cryogenic trapping.[4,6,12,13] This second trap, however, can also produce lose of analytes. Peng and Batterman[6] found that recoveries for low-boiling-point analytes (<60 °C) are <80%.

Recently, there has been much effort to develop an on-line system that allows near-real-time measurements in ambient air and gaseous samples.[14−21] The use of an on-line preconcentrator eliminates the errors associated with sample storage and provides rapid results that can help in a fast and appropriate response when a problem is detected.

On-line coupling is complicated as a result of the very strict requirement for a narrow injection bandwidth that permits the complete separation of the less retained compounds without the need for a second focusing device and the need for sufficiently high sampling flow rates that permits the preconcentration and analysis of samples at parts-per-billion and sub-parts-per-billion

* Corresponding author. E-mail: rdsacks@umich.edu.

(1) Manolis, A. *Clin. Chem.* **1983**, *29*, 5.
(2) Pleil, J.; Lindstrom, A. *Clin. Chem.* **1997**, *47*, 723.
(3) Edwards, R.; Jurvelin, J.; Koistinen, K.; Saarela, K.; Jantunen, M. *Atmos. Environ.* **2001** *35*, 4829.
(4) Dewulf J.; Van Langenhove, H. *J. Chromatogr., A* **1999**, *843*, 163.
(5) Dewulf J.; Van Langenhove, H. *Atmos. Environ.* **1997**, *31*, 3291.
(6) Peng, C.; Batterman, S. *J. Environ. Monit.* **2000**, *2*, 313.
(7) Van Winkle, M.; Scheef, P. *Indoor Air* **2001**, *11*, 49.
(8) Woolfenden, E. *J. Air Waste Manage. Assoc.* **1997**, *47*, 20.
(9) Cao, X.; Hewitt, C. *J. Chromatogr., A* **1994**, *688*, 368.
(10) Helming, D. *J. Chromatogr., A* **1996**, *732*, 414.
(11) Dettmer, K.; Knobloch, T.; Engewald, W. *Fresenius' J. Anal. Chem.* **2000**, *366*, 70.
(12) Van Es, A.; Janssen, H.; Cramers, C.; Rijks, J. *J. High Resolut. Chromatogr.* **1988**, *11*, 852.
(13) Baltusen, E.; David, F.; Janssen, H.; Cramers, C. *J. High Resolut. Chromatogr.* **1998**, *21*, 332.
(14) Mitra, S.; Yun, C. *J. Chromatogr.* **1993**, *648*, 415.
(15) Mitra, S.; Lai, A. *J. Chromatogr. Sci.* **1995**, *33*, 285.
(16) Mitra, S.; Xu, Y.; Chen, W.; Lai, A. *J. Chromatogr., A* **1996**, *727*, 111.
(17) Feng, C.; Mitra, S. *J. Chromatogr., A* **1998**, *805*, 169.
(18) Lu, C.; Zellers, E. *Anal. Chem.* **2001**, *73*, 3449.
(19) Lu, C.; Zellers, E. *Analyst* **2002**, *127*, 1061.
(20) Mitra, S.; Xu, Y.; Chen, W.; McAllister, G. *J. Air Waste Manage. Assoc.* **1998**, *48*, 743.
(21) Feng, C.; Mitra, S. *J. Microcolumn Sep.* **2000**, *12*, 267.

10.1021/ac020575+ CCC: $25.00
Published on Web 01/15/2003

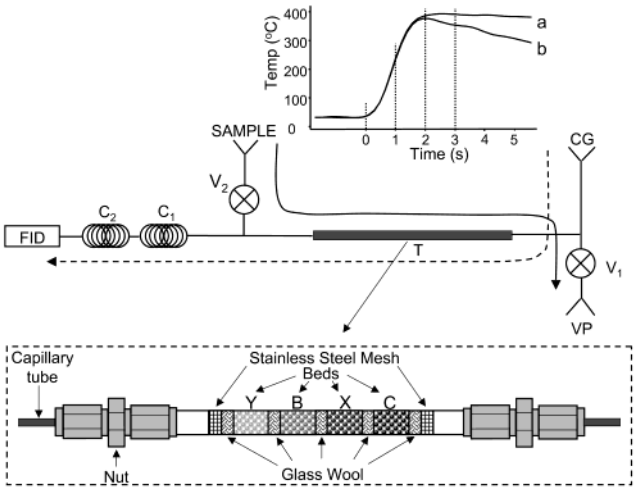

Figure 1. Experimental system used to evaluate performance of the multibed on-line sorption trap. Valves V_1 and V_2 are used to control the gas flow direction through the trap tube. The solid line from the sample source to the vacuum pump shows sample gas flow during preconcentration, and the dashed line shows carrier gas flow during desorption. Insets show details of the trap design and the temperature versus time profiles for a two-step heating pulse (a) and a single-step pulse (b). See text for details.

levels in relatively short times. Feng and Mitra[17] showed that the bandwidth of the desorbed compounds increases as the inside diameter of the adsorbent trap increases because heat transfer to the center of the trap during desorption is slower. The use of traps with 0.53-mm i.d. downstream from larger sampling beds results in injection peak widths of 1.2 and 1.5 s for methanol and acetone, respectively. However, the use of small-inside diameter traps increases pressure drop along the system and decreases the sampling flow rate in an on-line system. Lu and Zellers[19] found that bed masses >10 mg for 60/80 mesh Carbopack B limited the flow rate achievable to <0.1 L min^{-1} when a sampling pump was used and a 1.15-mm-i.d. glass tube was used as a trap.

Another inconvenience related with the use of sorbent traps is that no single sorbent material meets all the ideal criteria for preconcentrating VOCs from an air matrix. Thus, it is necessary to use multibed sorbent traps to preconcentrate a wide range of VOCs, which makes it necessary to determine both the correct mass of adsorption materials for each bed in a multibed trap[18,19] and their configuration to eliminate memory effects.

The work described here is part of a project devoted to the development of a portable GC instrument with an on-line preconcentration system that permits fast and accurate near-real-time analysis of VOCs in ambient air and gaseous samples, including static and dynamic headspace samples, auto exhaust samples, and diagnostic breath samples. The work described here is devoted to the evaluation of a multibed trap and the determination of the best operational conditions to obtain small injection plug bandwidths with minimal injection artifacts.

EXPERIMENTAL SECTION

Apparatus. Figure 1 shows the experimental platform developed for these studies. Insets show an enlarged drawing of the sorption trap and the heating pulse used for rapid desorption. A pair of low-dead-volume microvalves, V_1 and V_2 (model LFVA1230113H, The Lee Co., Westbrook, CT), is used to control the gas flows in the trap tube, T. The solid line from the sample source to vacuum pump, VP (model UN86KNI, KNF Newberger, Inc., Trenton, NJ), shows the sample gas flow path when both valves are open (sample preconcentration). The dashed line from the carrier gas supply, CG, to the flame ionization detector, FID, shows the carrier gas flow path when both valves are closed (sample injection and separation).

Table 1. Adsorbents Used in the Multibed Trap and Their Characteristics

symbol	adsorbent	mesh size	surface area (m^2 g^{-1})	density (g mL^{-1})	application
		Carbon Molecular Sieves			
C	Carboxen 1000	60/80	1200	0.44	C_2−C_5
		Graphitized Carbon			
B	Carbopack B	60/80	100	0.36	C_5−C_{12}
X	Carbopack X	40/60	250	0.41	C_3−C_5
Y	Carbopack Y	40/60	25	0.42	C_{12}−C_{20}

A series-coupled column ensemble consisting of a 10-m-long, 0.25-mm-i.d. fused-silica capillary with a 0.25-μm bonded film of poly(ethylene glycol) (Rtx-WAX, Restek Corp., Bellafonte, PA) followed by a 15-m-long, 0.25-mm-i.d. fused-silica capillary with a 0.5-μm bonded film of 5% phenyl dimethyl polysiloxane (Rtx-5, Restek), is used to achieve enhanced resolution of the early-eluting compounds in the test mixture. The columns are housed in the oven of a Varian 3700 GC (Varian Instruments, Walnut Creek, CA). The Varian FID was used without change.

Trap Design. An 80-mm-long, 1.35-mm-i.d. trap tube made of Inconel 600, a Ni−Co alloy (Accu-Tube Corp., Englewood, CO), contains the adsorbent materials as four discreet beds. This trap design is similar to a design by Lu and Zellers[18,19] for a trap in a glass tube. Adsorption beds labeled C, X, B, and Y correspond to the four commercial adsorption materials described in Table 1. About 2.2 mg of each material was used. This quantity is sufficient to prevent breakthrough of any of the target compounds at the concentrations used in this study.[18,19] The adsorption strength of the beds is graded, with bed C the strongest and Y, the weakest. During sample collection, flow is from left to right through the trap tube, and the higher-boiling-point compounds are quantitatively removed by the first bed(s) and, thus, never reach bed C, from which they would be very difficult to desorb as a narrow vapor plug. The beds are separated by glass-wool plugs, and stainless steel screens are used to confine the ends of the four-bed ensemble.

The trap is terminated at both ends with 0.25-mm-i.d. fused-silica tubing by means of low-dead-volume metal fittings. The fused-silica tube leading to the separation column is connected to a low-dead-volume all-glass splitter for connection with valve V_2 and the column ensemble. During sample collection (both valves open), the flow rate of sample gas through the trap was typically in the range of 50−100 cm^3/min, as determined by the vacuum pump pressure and the pneumatic restriction between the pump and the atmospheric pressure sample. A type-J thermocouple using 0.127-mm-i.d. wire (36 AWG, Omega Engineering, Stamford, CT) attached to the outer wall of the tube is used to monitor the trap temperature. The very fine wire (low thermal mass) minimizes response delay. Total dead volume downstream

Table 2. Volatile and Semi-Volatile Compounds Used in Test Mixtures

peak	compd name	bp, °C	peak	compd name	bp, °C	peak	compd name	bp, °C
1	acetaldehyde	21	17	2-pentanone	100−101	32	1,2,4-trimethylbenzene	168
2	methanol	64.7	18	2,5-dimethylfuran	93	33	benzaldehyde	178−179
3	pentane	35−36	19	1-butanol	117.7	34	limonene	175.5
4	isoprene	34	20	toluene	110.6	35	1,2,3-trimethylbenzene	175−176
5	acetone	56.2	21	octane	125−127	36	1,2-dichlorobenzene	180
6	ethanol	78	22	hexanal	131	37	phenol	182
7	2-propanol	82.4	23	*n*-butyl acetate	126.1	38	dodecane	216.3
8	hexane	69	24	ethylbenzene	136.2	39	3-pentanone	102
9	butanone	80	25	*m*-xylene	139.1	40	1-pentanol	136−138
10	ethyl acetate	77.1	25	*p*-xylene	138.3	41	2-heptanone	149−150
11	1-propanol	97	26	nonane	150.8	42	undecane	196
12	2-butanol	98	27	*o*-xylene	143−145	43	bromobenzene	156
13	chloroform	61	28	cumene	152−154	44	dichloromethane	39.8
14	benzene	80.1	29	α-pinene	155	45	trichloroethylene	86.7
15	isooctane	98−99	30	*β*-pinene	167	46	dimethyl sulfide	37.3
16	heptane	98.4	31	decane	174			

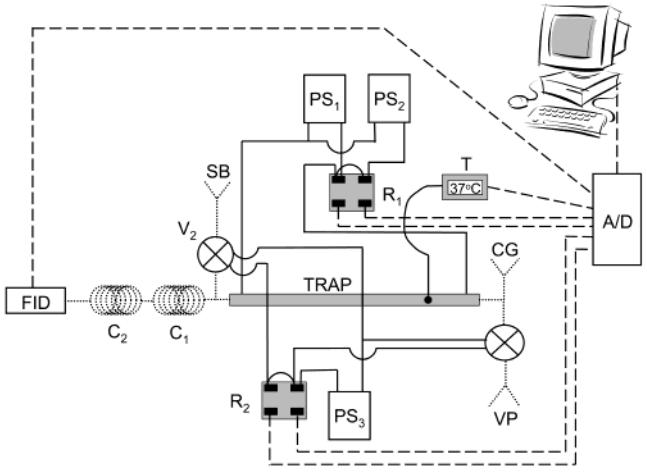

Figure 2. Schematic representation showing circuitry used for operation of the flow control valves and trap heating cycle. R_1 and R_2 are solid-state relays, PS_1 and PS_2 are power supplies used for trap heating, and PS_3 is the valve-driver power supply.

from the bed ensemble during sample desorption is estimated at ~14 μL.

Figure 2 shows the electric circuitry used for trap heating, valve control, and data acquisition. The trap tube is resistively heated by a two-step heating process using a relatively high-current, short-duration pulse for rapid heating and a longer-duration, lower-current pulse to maintain a constant operating temperature for several seconds. Solid-state relays, R_1 and R_2, are used to control trap heating and valve operation, respectively, by means of a 16-bit A/D board (CIO-DAS16/F, Measurement Computing Corp., Middleboro, MA). A 12-V dc supply PS_3 (model XP-603, Elenco Electronics, Wheeling, IL) is used as a valve driver. Adjustable autotransformers PS_1 and PS_2 provide ac power for trap heating, since the very low resistance of the trap tube (0.48 Ω) made the use of a dc supply more difficult. Typically, the higher current from PS_1 is applied for 0.9 s for very rapid heating with minimal overshoot, and the lower current from PS_2 is used to maintain the trap temperature for 10 s to ensure complete desorption of the sample and to minimize contamination of the trap by traces of high-boiling-point impurities in the sample. The values of the ac voltages were adjusted to vary the desorption temperature. Trap temperature versus time with (a) and without (b) the lower current pulse is shown in the inset of Figure 1.

Materials and Procedures. Table 2 lists the test compounds and their boiling points. Samples were prepared in 12-L Tedlar gas sampling bags (SKC Inc., Eighty Four, PA) by injecting microliter quantities of mixtures or individual components and diluting with dry air. Vapor concentrations in the range of 8−35 ppm (v/v) were used. For all studies, sample collection times in the range of 2−20 s were used with a sample gas flow rate of 50 cm^3/min.

Hydrogen carrier gas was purified with filters for moisture, hydrocarbons, and oxygen. The inlet pressure was 25.4 psia. For measurements of the injection plug width, the gas chromatographic column ensemble was replaced with a 55-cm-long segment of 0.1-mm-i.d. deactivated fused-silica tubing, which has nearly the same pneumatic restriction as the column ensemble. Since the holdup time of this restrictor is only 2.0 s, vapor plugs injected from the sorption trap can be examined under realistic conditions. Erratic results were observed if the trap heating cycle was initiated within a few seconds after closing the flow control valves, and a 60-s delay was used in all cases to ensure complete carrier-gas flow stabilization.

RESULTS AND DISCUSSION

General Operating Characteristics. An important consideration in trap design is the amount of sample vapor that can be retained by the trap and the time that the sample can be retained before breakthrough results in sample loss from the trap. Feng and Mitra[17] and Lu and Zellers[18,19] have studied breakthrough for several adsorbent materials. Breakthrough volumes for 1.0 ppm acetone and 2-propanol for a 2-mg bed of Carboxen 1000 were reported to be ~2 L.[18] Data from these reports were used as a basis for the selection of the bed masses to minimize the risk of sample loss for the concentration ranges, sampling times, and sampling flow rates used in this study. However, a larger number of compounds was used in the present study, and for most of them, no breakthrough data are available.

Although a greater bed mass allows for larger samples to be collected without breakthrough, a larger bed generally results in a broader injection plug and, thus, reduced resolution, particularly for early eluting compounds. Since the multibed adsorption trap

is used directly as the GC inlet without further injection plug focusing, a total bed mass of less than ~10 mg is desirable. In addition, for a fixed trap inside diameter, increasing the bed mass results in an increase in bed length and, thus, a decrease in sampling flow rate for a fixed pressure drop.

Breakthrough volumes are also dependent on temperature during sample collection. Mitra et al.[17] modeled trap performance as a small (low resolution) separation column and showed that the log of the breakthrough time is proportional to the reciprocal of the trap temperature. Although the operation of sorption traps at subambient temperatures does reduce the risk of breakthrough, it is inconvenient and was not used in this study. For most of the compounds considered in this study, the bed mass should provide for quantitative analyte collection at room temperature (22 °C).

For the four-bed graded trap, during sample preconcentration, each sample component migrates through the trap until it reaches the bed with adequate strength for quantitative adsorption of that component for the duration of the sampling interval. Thus, narrower, better-defined bands of trapped sample should be formed for the different mixture components than can be obtained with a single-bed trap using a mixture of the adsorbent materials. This was confirmed in preliminary studies.

During sample preconcentration, the highest-boiling-point components are trapped in the first adsorbent encountered, which is the weakest adsorbent. For injection, the flow is reversed, and the highest-boiling-point components are released into the carrier gas flow exiting the trap. Thus, these sample components never contact the stronger adsorbents from which they would be difficult to desorb as a narrow plug. This results in much improved peak shapes. Feng and Mitra[20] and Lu and Zellers[19] described multibed traps with flow reversal after sample collection to protect a graphite-molecular-sieve trap from high-boiling-point compounds.

Figure 3 shows chromatograms for the first 42 components in the test mixture, illustrating the initial chromatogram and trap memory effects for the case when the trap is operated in the normal configuration, with the weakest adsorbent upstream during preconcentration and downstream during injection [a and b], and for the case when the trap is operated in the reverse configuration, with the strongest adsorbent upstream during preconcentration and downstream during injection [c and d]. Chromatograms a and c were obtained from the first heating cycle, and the memory effects shown in chromatograms b and d are from a second trap-heating cycle several minutes later after completion of the initial chromatograms. Note that no flow reversal was used between the two heating cycles. Peak numbers correspond to component numbers in Table 2. The experiments for the two cases were performed on different days with different test mixtures containing the same compounds but with different concentrations. All concentrations, however, were in the 8−35 ppm range. A sample collection time of 12.0 s was used with a sample gas flow rate of 0.83 cm^3/s (50 cm^3/min). For sample injection, the trap was heated to 300 °C. The chromatograms were obtained with an initial 2.0-min isothermal interval at 30 °C, followed by a 15 °C/min temperature program to 150 °C.

The chromatogram is complete in less than 550 s, and when the trap is operated in the normal configuration, relatively symmetric peaks are observed for most components. The second heating cycle [Figure 3b] results in a nearly flat baseline with no

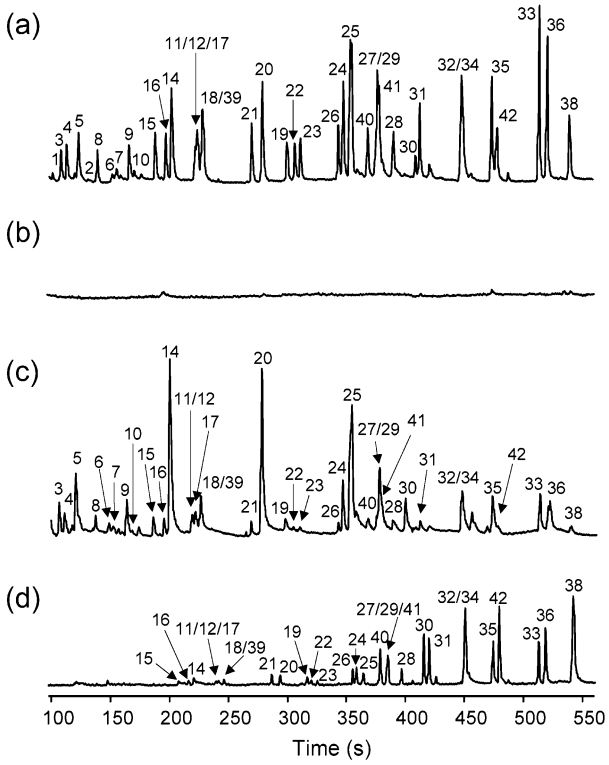

Figure 3. Chromatogram showing the analysis of the first 42 components in Table 2: (a) initial chromatogram for normal trap configuration, (b) memory effect chromatogram for normal trap configuration, (c) initial chromatogram for reverse trap configuration, and(d) memory effect chromatogram for reverse trap configuration. Numbers by peaks correspond to the component numbers in Table 2.

significant peaks, indicating that the sample was quantitatively desorbed from the trap during the first heating cycle.

When the trap is operated in the reverse configuration, many peaks in the chromatogram from the first heating cycle are more severely tailed and diminished in area relative to the case when the trap is operated in the normal configuration. This is particularly apparent for the higher-boiling point components appearing late in the chromatogram shown in Figure 3c.

For the second heating cycle with the trap operated in the reverse configuration, a large memory effect is observed in the chromatogram, as seen in Figure 3d. The early-eluting peaks for the lower-boiling-point components show relatively small memory effects, since these compounds are more easily desorbed from the Carboxen 1000 (strongest adsorbent). For the later-eluting peaks in chromatogram 3d, very large memory effects are observed, and it is apparent that these components are not easily desorbed from Carboxen 1000, even at temperatures of 300 °C. When the trap is operated in the reverse configuration, it is likely that the entire mixture is adsorbed (assuming no breakthrough) by the Carboxen 1000, which is the upstream bed during sample preconcentration.

The different heating profiles shown as insets to Figure 1 were compared for the normal trap configuration, and no significant differences in were observed in the chromatograms from the test mixture or from the memory-effect chromatogram. Thus, the low-current power supply used to maintain the trap temperature for the duration of the heating cycle appears unnecessary. However,

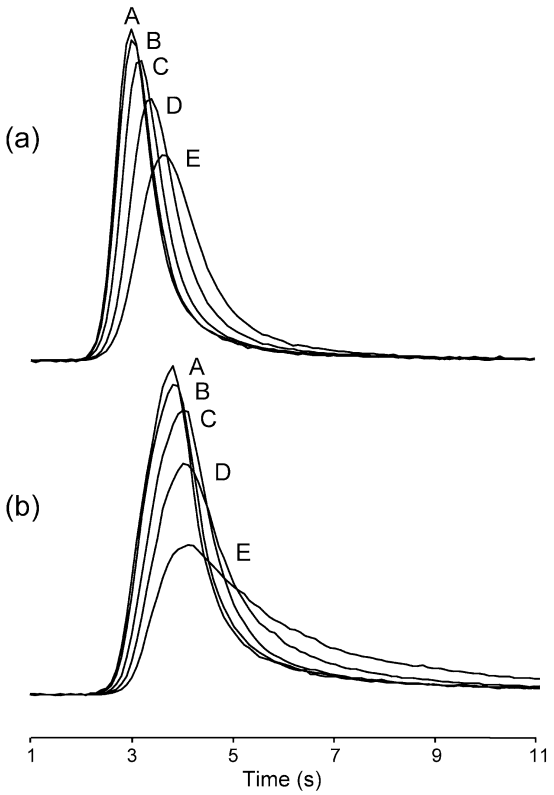

Figure 4. Injection plug profiles for *n*-pentane (a) and *n*-decane (b) for trap temperatures of 385 (A), 350 (B), 300 (C), 250 (D), and 200 °C (E).

the low-current sustained heating was used to reduce the risk of gradual accumulation in the trap of high-boiling-point impurities in the sample gas.

Injection Plug Characteristics. Injection plug width is a critical issue if the sorption trap is to be used on line as a GC injection device. Injection-plug widths depend of many factors, including the distribution of the analytics along the multibed trap, the heating rate, peak temperature, and heating pulse duration. Heating usually is provided by heaters external to the trap tube, and heat conduction through the tube and the sorbent beds is an important consideration. The gas transport rate and dead volumes downstream from the trap are important issues.

For these studies, the separation column was removed and replaced with a deactivated fused-silica restrictor with a holdup time of 2.0 s. The restrictor was maintained at a temperature of 120 °C. Figure 4a shows injection plugs for *n*-pentane, and Figure 4b shows injection plugs for *n*-decane. Traces A, B, C, D, and E correspond to injection temperatures of 385, 350, 300, 250, and 200 °C, respectively. The dry air sample contained ~20 ppm (v/v) of the analyte. A 4.0-s sampling interval was used at a flow rate of 1.25 cm^3/s.

For *n*-pentane, the injection plug width (full width at half-height) decreases from 1.3 s at 200 °C to 0.7 s at 385 °C, and the plug apex is shifted ~0.6 s to early time. Note that the adsorbents used in this study are all stable to at least 400 °C. At all injection temperatures used in this study, the injected vapor plugs for *n*-pentane are quite symmetrical. For *n*-decane, the injection plug width decreases from 2.3 s at 200 °C to 1.0 s at 385 °C, and the plug apex is shifted ~0.3 s to early time. At all temperatures, the

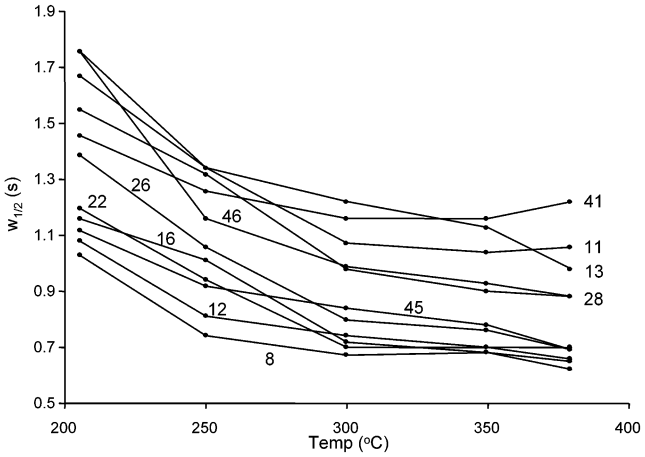

Figure 5. Plots of injection plug width (full width at half-height) versus trap temperature. Numbers by the plots correspond to the component numbers in Table 2.

injection plugs from *n*-decane show significantly more tailing than the plugs from *n*-pentane, and the tailing is quite severe for injection temperatures <300 °C. Note that during the initial isothermal interval at 30 °C, significant on-column focusing occurs for the high-boiling-point components in the injection plug,[19] and this relaxes the need for very narrow injection plugs.

Figure 5 shows plots of injection plug width versus trap injection temperature for a number of the target compounds from Table 2. These compounds span a wide range of boiling points and functionalities. Numbers by the plots correspond to the component numbers in Table 2. Experimental conditions are the same as for Figure 4. For all of the compounds, injection-plug peak area is independent of desorption temperature for the temperature range shown in Figure 5. This suggests quantitative recovery and is consistent with the memory-effect data in Figure 3. For most of the compounds, the injection plug width decreases steadily with increasing temperature, but the rate of decrease is relatively small for temperatures above ~300 °C. For temperatures of 300 °C and greater, most of the compounds produce injection plug widths in the range from ~0.7−1.3 s.

In general, the injection plugs widths reported here are substantially smaller than previously reported values for on-line sorption traps. Feng and Mitra[21] reported injection-plug width of ~1.5 s for toluene using a 0.53-mm-i.d. silica-lined stainless steel trap. Wider plugs were obtained for larger-inside-diameter traps, which may be the result of increased dead volume and slower heating. Lu and Zellers reported injection plug widths in the range of 1−3 s for several adsorbents, including Carboxen 1000, used in single-bed 1.15-mm-i.d. glass traps[18] and in a multibed trap operated with a reversal in the gas flow direction between sample collection and injection, similar to the system described here.[19] The smaller injection plug widths observed in the present study may be the result of using a metal trap tube and the more rapid heating obtained with the dual power supply used in this study. Some of the components in Table 2 decompose during desorption at the higher temperatures. This is discussed in the following section.

The injection plug width for the sorption trap depends on both the rate of desorption and the rate of transport. Vapor transport is determined by the volumetric flow rate during desorption and

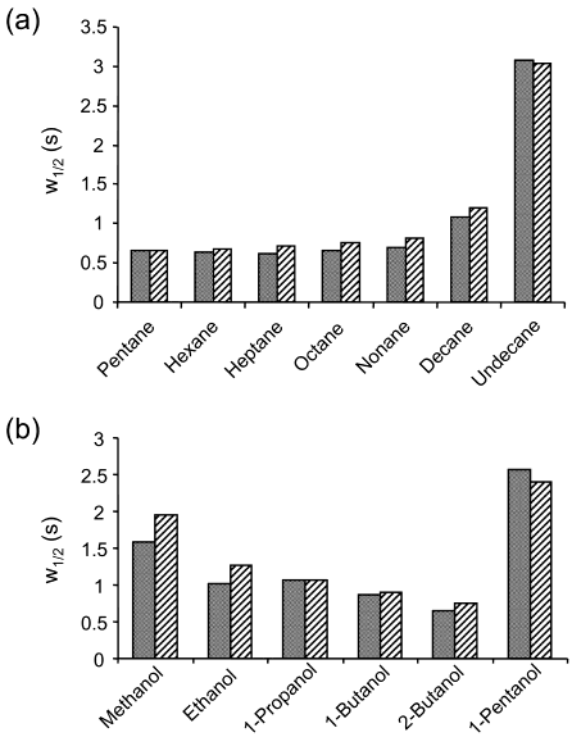

Figure 6. Injection plug widths for *n*-alkanes (a) and alcohols (b) for trap temperatures of 385 (solid gray bars) and 350 °C (bars with diagonal lines).

by the dead volumes in the downstream end of the trap and the tubing and fittings connecting the trap to the separation column. The carrier gas flow through the trap during desorption is 1.7 cm^3/min (column flow), and the dead volume is estimated at 14 μL. This gives a dead time of ~0.5 s. The fact that the injection plug widths in Figure 5 become relatively independent of trap temperature for temperatures above about 300 °C with minimum values about 0.6 s suggests that further reductions in injection plug widths will require smaller dead volumes or higher flow rates.

Figure 6 shows the effects of component volatility and polarity on injection plug width for *n*-alkanes (a) and for alcohols (b). The solid gray bars are for an injection temperature of 385 °C and the bars with diagonal lines are for an injection temperature of 350 °C. Sample concentrations and flow conditions during preconcentration are the same as for Figure 4. For the alkanes, injection plug widths show a very gradual increase with increasing molecular weight (decreasing volatility) for *n*-pentane through *n*-nonane and then increase more rapidly for *n*-decane and much more rapidly for *n*-undecane. This appears to set a lower limit on component volatility if relatively narrow injection plugs are to be obtained. This limit may be extended by taking advantage of on-column focusing for temperature-programmed applications. Note in the chromatogram in Figure 3a that the peak for *n*-dodecane (peak 38) shows no sign of excessive broadening or tailing.

A very different situation is observed for the polar alcohols. Methanol, which is the most hydrophilic of the alcohols and the most hydrophilic compound in the test mixture, produces a relatively large injection plug width. This may be the result of greater dipole interactions and possible hydrogen bonding with the adsorbents or traces of water vapor from the sample. This could reduce the rate of desorption from the bed and the rate of

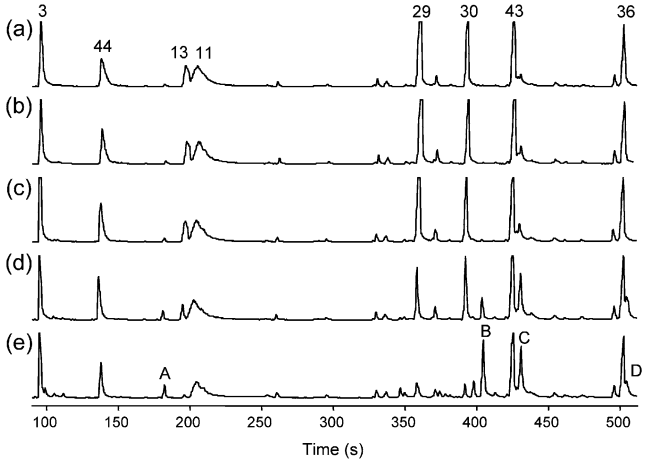

Figure 7. Chromatograms showing decomposition of thermally labile compounds. The trap temperatures were 200 (a), 250 (b), 300 (c), 350 (d), and 385 °C (e). Peak numbers correspond to component numbers in Table 2. Peaks identified with letters are decomposition products.

migration through the bed during the heating cycle. As the hydrophilicity of the alcohols decreases with increasing molecular weight, the injection plug width steadily decreases, and 2-butanol has an injection plug width of ~0.7 s, which is about the same as for *n*-pentane. For 1-pentanol, the injection plug width increases to ~2.6 s, and this is probably the result of decreased volatility. Thus, both volatility and polarity are determinants of injection plug width.

Sample Decomposition. At the higher desorption temperatures required to obtain narrower injection plugs, sample decomposition during trap heating becomes an important issue. Decomposition of thermally sensitive compounds may be facilitated by the hot metal trap wall and by the adsorbent materials themselves. The decomposition of α-pinene on solid sorbents including Carboxen was reported by Coeur et al.[22] The decomposition mechanism is not well understood but may involve traces of active species such as NO_x and ozone. Cao and Hewitt[23] reported complete decomposition of α-pinene and β-pinene on a Carbotrap bed with a desorption temperature of 220 °C.

Figure 7 shows chromatograms of some of the test components using desorption temperatures of 200 (a), 250 (b), 300 (c), 350 (d), and 385 °C (e). Peak numbers correspond to component numbers in Table 2. For desorption temperatures up to 300 °C, the desorption temperature has little effect on the qualitative features of the chromatograms, except that peak 44 (dichloromethane) is significantly narrower at the higher desorption temperatures. A relatively broad and significantly tailed peak is observed for 1-propanol (peak 11) for all desorption temperatures. This is characteristic of all alcohols on poly(ethylene glycol) columns.

For desorption temperatures of 350 and 385 °C, large decreases in peak area are observed for peaks 13 (chloroform), 29 (α-pinene), and 30 (β-pinene). In addition, new peaks appear in the chromatograms. These are labeled A−D in chromatogram e. No attempt was made to identify these compounds, which are assumed to be decomposition products. Very small peaks for

(22) Coeur, C.; Jacob, V.; Denis, I.; Foster, P. *J. Chromatogr., A* **1997**, *786*, 185.
(23) Cao, X.-L.; Hewitt, C. *Chemosphere* **1993**, *27*, 695.

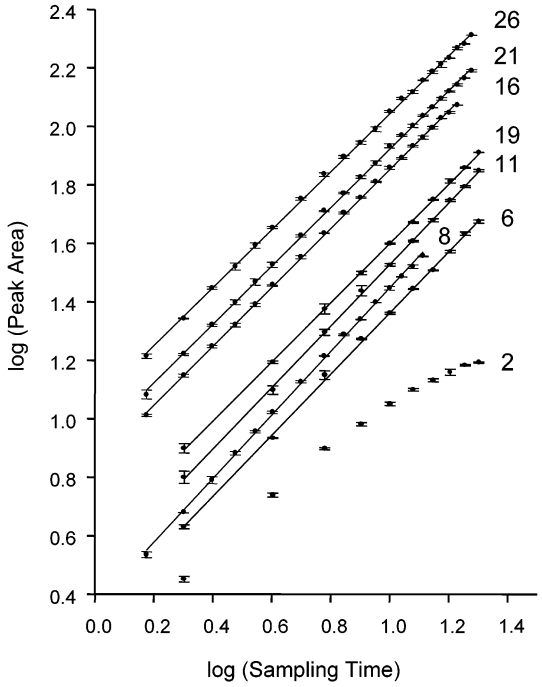

Figure 8. Plots of log peak area versus log sampling time. Numbers by plots correspond to component numbers in Table 2. Statistical data for the plots are found in Table 3.

components A and C are observed in chromatograms a and b for the lower-temperature desorption cases, and it is not known if these peaks are from decomposition products or impurities in the sample. This study suggests that desorption temperatures much greater than 300 °C should be avoided when these more labile components are present in the sample mixture. However, since little reduction in injection-plug widths is obtained with desorption temperatures greater than 300 °C (see Figure 5), sample decomposition can be minimized with little loss in trap performance.

Quantitative Analysis. The mass of analytes collected in the trap can be changed by changing the sample collection time, the sample flow rate during preconcentration, or the sample concentration. The sample collection time is most easily changed and avoids issues of sample loss from permeation and wall adsorption in the gas-sampling bag for very low concentration samples. Figure 8 shows plots of log peak area versus log sampling time for several components in the test mixture. Plot numbers correspond to the component numbers in Table 2. The sample flow rate was 1.33 cm^3/s (80 cm^3/min). Sampling times ranged from 2.0 to 20 s. The trap was heated to 300 °C for sample injection.

With the exception of the plot for methanol, which is nonlinear over the entire range of sample collection times, the plots are all very linear. Table 3 summarizes the statistical data for the plots. Again, with the exception of methanol (plot 2), the log−log correlation coefficients (r^2) are all >0.999. The log−log slopes are in the range of 0.99−1.06, indicating very good peak-area linearity with the mass of analyte challenging the trap. The error bars in Figure 8 are standard deviation for three replicate samples. Again, very good shot-to-shot reproducibility is indicated. Relative standard deviations are all <5% and typically in the range 1−3%.

The nonlinear plot obtained for methanol is probably the result of sample breakthrough caused by the very polar nature of methanol and the relatively nonpolar surface of the carbon-based adsorbent materials used in the trap. Solvation of methanol by traces of water vapor in the sample may also contribute to sample breakthrough. Note that ethanol (plot 6) and 1-propanol (plot 11) produce very linear plots with log−log slopes similar to the nonpolar components in the mixture.

Table 3. Slopes and Correlation Coefficients for the Plots in Figure 8

peak	compd name	slope	R^2
6	ethanol	1.05 ± 0.01	0.9998
8	hexane	1.06 ± 0.02	0.9991
11	1-propanol	1.01 ± 0.01	0.9998
16	heptane	1.01 ± 0.01	0.9998
19	1-butanol	1.05 ± 0.02	0.9993
21	octane	1.00 ± 0.01	0.9997
26	nonane	0.99 ± 0.01	0.9995

CONCLUSIONS

The graded, multibed adsorption trap is a very effective on-line preconcentration device for the gas chromatographic analysis of airborne organic compounds for sample collection times up to at least 20 s. The flow direction reversal between sample collection and injection into the chromatographic column is essential to achieve narrow injection plugs with minimal tailing. With flow reversal, no memory effects are observed, and quantitative recovery of all mixture components except methanol is observed. The more rapid heating with minimal overshot obtained with the dual-power-supply operation results in substantially more rapid heating and narrower injection plugs than with previously described on-line sorption traps. Alternative trap designs, which reduce dead volume and increase volumetric flow rate during desorption are under investigation.

The compound volatility range for the sorption trap device is limited to about C_{12} hydrocarbons and C_5 alcohols. Less volatile compounds produce injection plug width of over 2 s, and this can result in substantial reductions in chromatographic resolution. However, for temperature-programmed separations, on-column focusing of the less volatile compounds may extend the volatility range of the device. For compounds that do not thermally degrade during desorption, higher desorption temperatures can be used, which may extend the volatility range to higher-molecular-weight compounds. However, the adsorption materials used in the trap may be thermally altered at temperatures >400 °C.

A major advantage of the preconcentrator described in this report is that it is operated on-line without the need for a conventional GC inlet. This obviates the need for additional focusing devices, inlet splitters, and temperature-programmed operation. The on-line sorption trap should be useful for a variety of applications, including ambient air and workplace air monitoring, the analysis of gasoline-range hydrocarbons from auto exhaust, static and dynamic headspace analysis, and diagnostic breath analysis.

ACKNOWLEDGMENT

The technical assistance of Dr. Edward Zellers and Dr. Chia-Jung Lu, School of Public Health, University of Michigan, for design of the sorption trap is gratefully acknowledged. Juan M. Sanchez acknowledges the Spanish Ministry of Education for the

financial support of his postdoctoral stay at the University of Michigan (Ref. Ex2001 40521369). Funding for this work was provided by Grant no. R01-OH03692 from the National Institute for Occupational Safety and Health of the Centers for Disease Control and Prevention (NIOSH-CDCP). Additional support provided by the University of Michigan Center for Wireless Integrated Microsystems (WIMS) through the Engineering Research Centers Program of the National Science Foundation under Award no. EEC-9986866 is also gratefully acknowledged.

Received for review September 16, 2002. Accepted November 20, 2002.

AC020575+